Supporting Information

Competing with other polyanionic cathode materials for potassium-ion batteries via fine structure design: A new layered $KVOPO_4$ with a tailored particle morphology

Jiaying Liao, Qiao Hu, Bo Che, Xiang Ding, Fei Chen, Chunhua Chen*

CAS Key Laboratory of Materials for Energy Conversions, Department of Materials Science and Engineering & Collaborative Innovation Center of Suzhou Nano Science and Technology, University of Science and Technology of China, Hefei 230026, Anhui, China

Corresponding authors: E-mail: cchchen@ustc.edu.cn; Phone: +86-551-63606971; Fax: (+86)551-63601592.

Table S1. The hydrothermal conditions and results.

Precursor (in 50 ml H_2O)		Products	Morphology
2mmol VO_2, 5mmol H_2SO_4	6mmol KH_2PO_4	$K_{0.5}VOPO_4 \cdot 1.5H_2O$	bulk
2mmol VO_2, 5mmol H_2SO_4	6mmol $K_2HPO_4 \cdot 3H_2O$	$K_{0.5}VOPO_4 \cdot 1.5H_2O$	nanosheets
2mmol VO_2, 5mmol H_2SO_4	3mmol $K_2HPO_4 \cdot 3H_2O$, 3mmol $K_3PO_4 \cdot 3H_2O$	$K_{0.5}VOPO_4 \cdot 1.5H_2O$	flower-like micro-sphere
2mmol VO_2, 5mmol H_2SO_4	6mmol $K_3PO_4 \cdot 3H_2O$	blue gel	-
4mmol VO_2, 10mmol H_2SO_4	12mmol $K_2HPO_4 \cdot 3H_2O$	$K_2(VO)_2(HPO_4)_3 \cdot 1.125H_2O$	rod

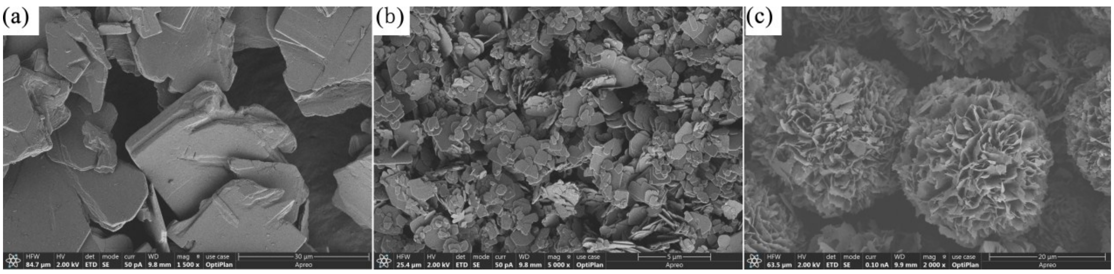

Fig. S1. SEM images of hydrothermal products: (a) bulk; (b) nanosheets; (c) micro-sphere.

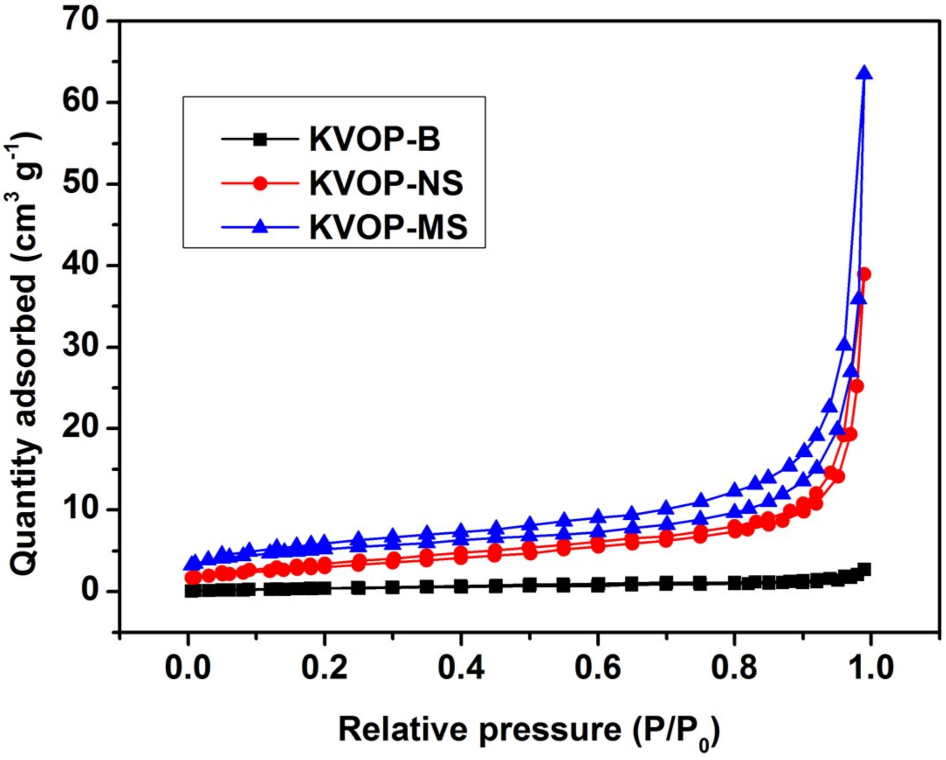

Fig. S2. N_2 adsorption-desorption isotherms KVOP samples.

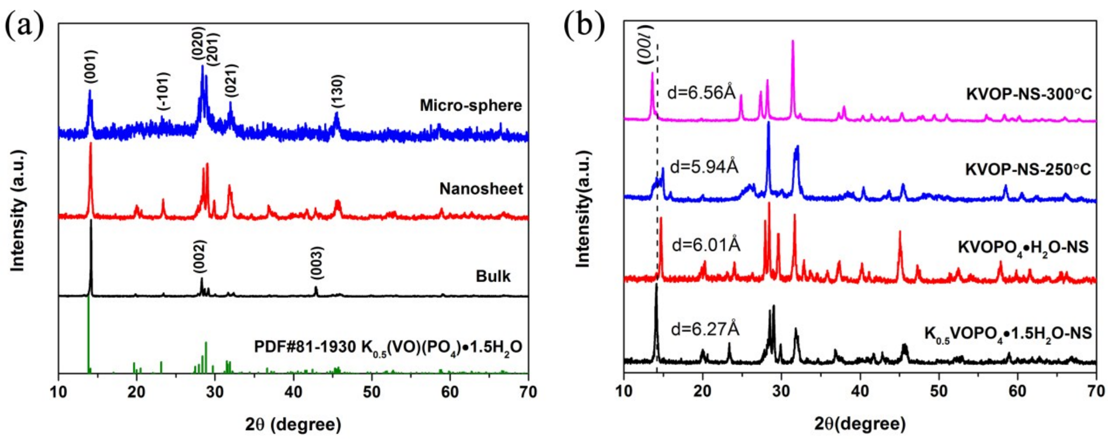

Fig. S3. XRD patterns of hydrothermal products (a) and KVOP-NS at different stages of the synthetic process (b).

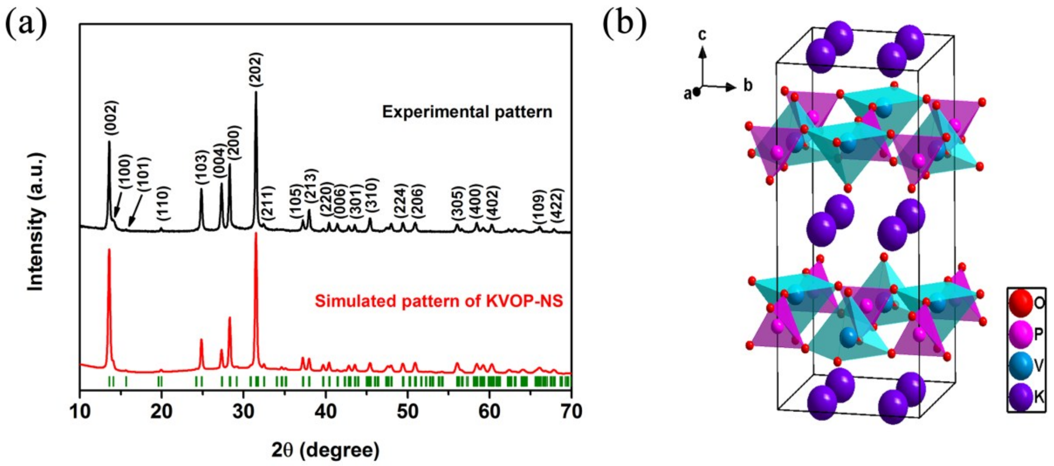

Fig. S4. (a) XRD and Rietveld refinement of the KVOP-NS ($P4_2mc$). (b) Representation of α_{II}-$KVOPO_4$ structure (The K position was not accurately refined due to the large relative errors).

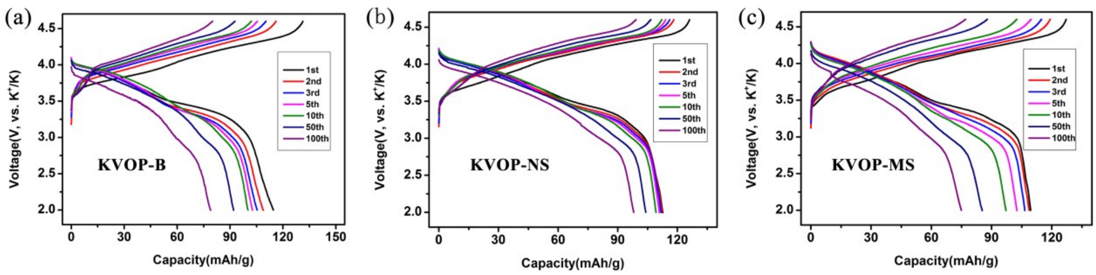

Fig. S5. Charge-discharge curves of the selected cycles of KVOP samples in 0.5 M KPF_6-PC/FEC (1/1, v/v) at a current density of 0.5C (1C=120 mAh/g): (a) KVOP-B; (b) KVOP-NS; (C) KVOP-MS.

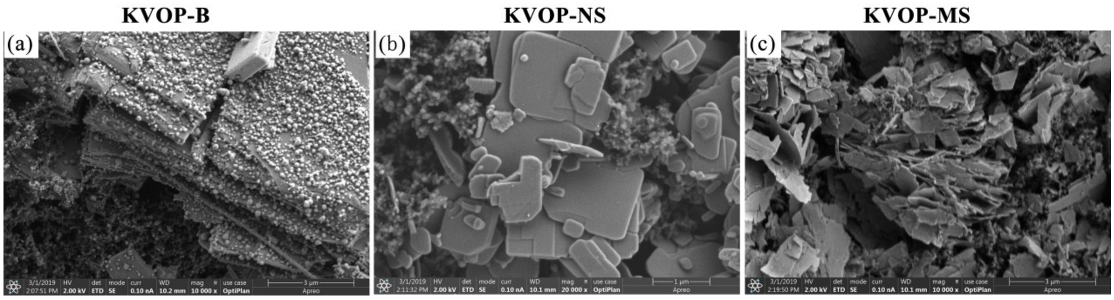

Fig. S6. SEM images of KVOP samples after cycling: (a) KVOP-B, (b) KVOP-NS, (c) KVOP-MS.

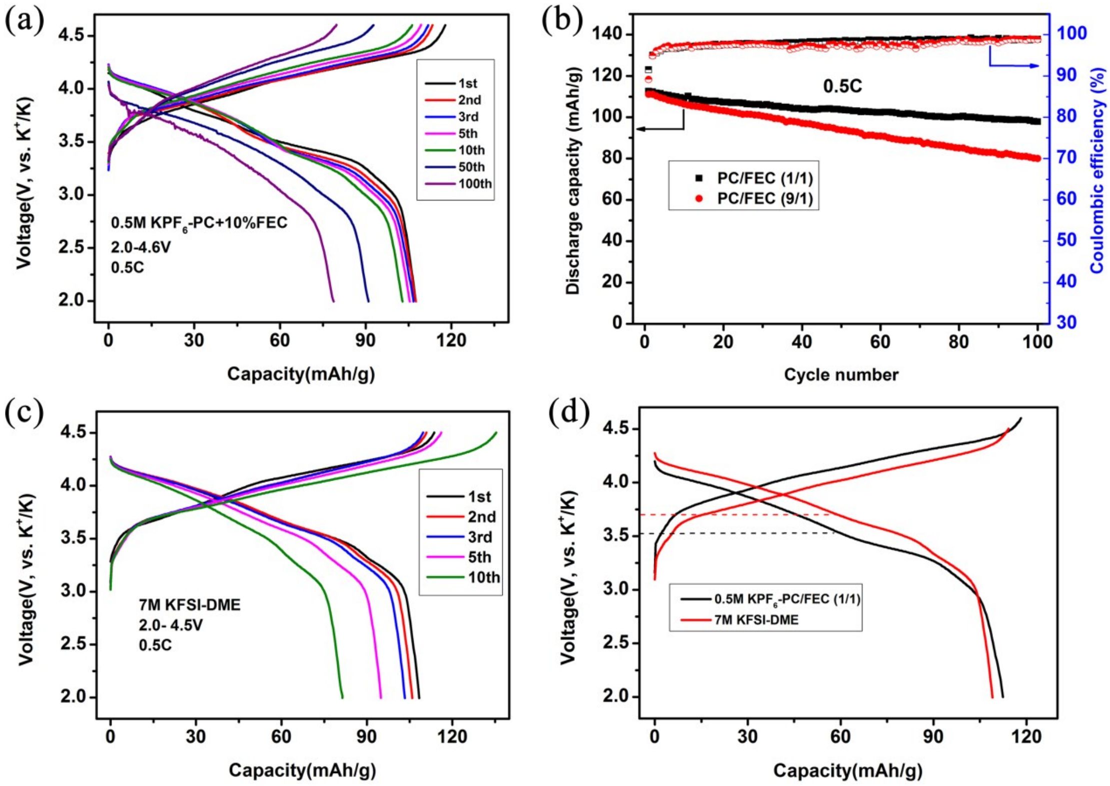

Fig. S7. (a) Charge-discharge curves of the selected cycles of KVOP-NS in 0.5 M KPF_6-PC/FEC (9/1, v/v) at a current density of 0.5C; (b) Comparison of cycling performance of KVOP-NS in 0.5 M KPF_6-PC/FEC (1/1) and 0.5 M KPF_6-PC/FEC (9/1); (c) Charge-discharge curves of the selected cycles of KVOP-NS in 7 M KFSI-DME at a current density of 0.5C; (d) Comparison of the initial charge-discharge profiles in 0.5 M KPF_6-PC/FEC (1/1) and 7 M KFSI-DME.

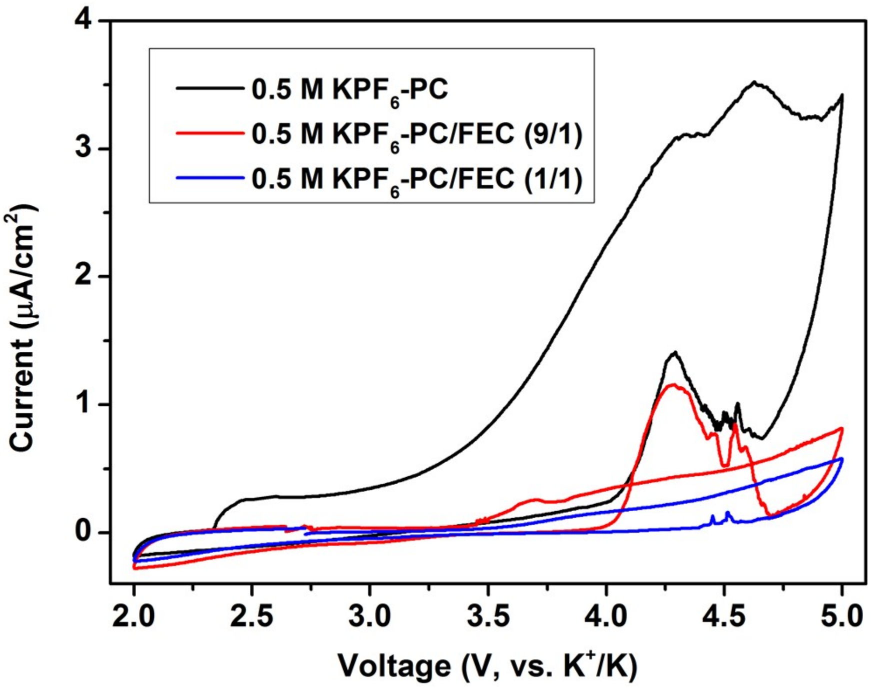

Fig. S8. CV curves of potassium half cells using aluminum foil as counter electrode in different electrolytes from 2.0 to 5.0 V at a scan rate of 0.1 mV s^{-1}.

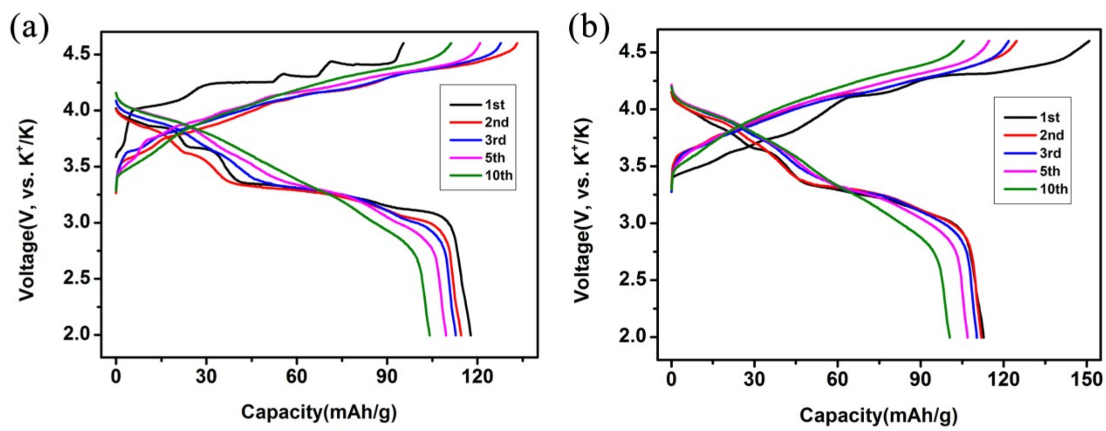

Fig. S9. Charge-discharge curves of the selected cycles of $K_{0.5}VOPO_4 \cdot 1.5H_2O$ (a) and $KVOPO_4 \cdot H_2O$ (b) nanosheets in 0.5 M KPF_6-PC/FEC (1/1, v/v) at a current density of 0.5C.

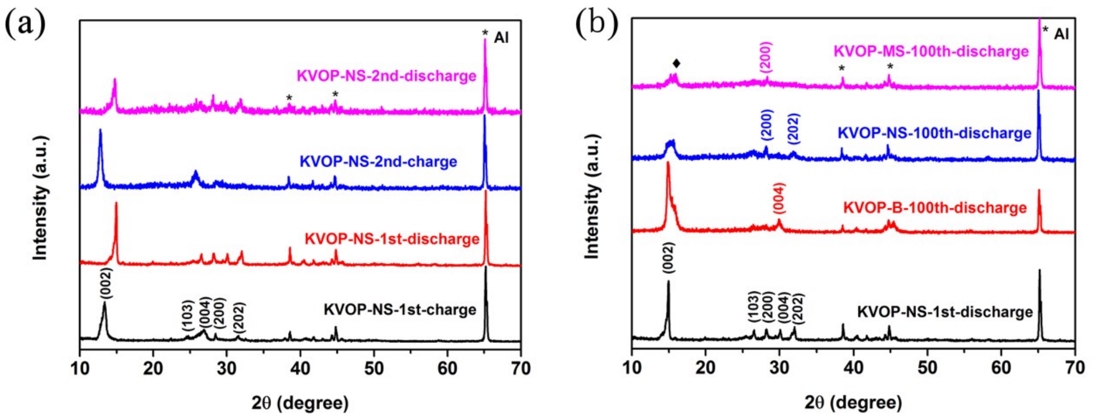

Fig. S10. Ex-situ XRD patterns of KVOP-NS after the 1st and 2nd cycles (a) and KVOP samples after 100 cycles (b).

Table S2. The detailed information of electrochemical section of various polyanionic cathodes in PIBs.

Composition	Electrolyte	Current collector	Voltage range	Cycle stability	Initial CE	References
$KVPO_4F$	0.7 M KPF_6-EC/DEC	Al	3.0-5.0 V	75% (30 cycles)	73%	[8]
$K_2[(VO)_2(HPO_4)_2C_2O_4]$	0.1 M $KClO_4$-PC	Al	2.0-4.6 V	83% (200 cycles)	79%	[11]
α-$KVOPO_4$	0.7 M KPF_6-EC/DEC	Al	2.0-4.8 V	~100% (50 cycles)	46%	[26]
	1 M KPF_6-PC		2.0-5.0 V	-	64%	
$KFeSO_4F$	0.1 M $KClO_4$-PC	Al	2.0-4.5 V	-	86%	[37]
$FePO_4$	1 M KPF_6-EC/EMC	Al	1.5-3.5 V	80% (50 cycles)	-	[38]
$K_3V_2(PO_4)_3$	0.8 M KPF_6-EC/DEC	Cu	2.5-4.3 V	96% (100 cycles)	70%	[39]
KVP_2O_7	0.5 M KPF_6-EC/DEC	Al	2.0-5.0 V	83% (100 cycles)	71%	[40]
$K_3V_2(PO_4)_2F_3$	1 M KPF_6-EC/PC	Al	2.0-4.6 V	97% (100 cycles)	73%	[41]
Layered $KVOPO_4$	0.5 M KPF_6-PC/FEC (1/1, v/v)	Al	2.0-4.6 V	87% (100 cycles)	91%	This work